Supplemental Data

Supplemental Methods

Coculture of macrophages with highly-apoptotic cells

Primary bone marrow cells were collected from 4-8wk old male C57BL/6J mice via hind limb flush with αMEM (L-glutamine, 10% FBS). Addition of murine M-CSF (30ng/mL, eBioscience #14-8983-80) induced differentiation of bone marrow-derived macrophages (MΦ). After 7d in culture, macrophages were plated independently at $1.5x10^6$ cells/well in αMEM (L-glutamine, 0.25% FBS) for coculture experiments. Bone marrow stromal cells (BMSCs) were isolated from bone marrow flush and cultured in αMEM (L-glutamine, 20% FBS) containing 10nM dexamethasone (Sigma). RM1-iC9, RM1, PC3, BMSC, MC4, BMC (total bone marrow cells) and MPEC cells were exposed to UV light for 30min to induce apoptosis. Cell death was confirmed via trypan blue incorporation. Highly-apoptotic (HA) cells (>90% trypan blue incorporation) were plated in coculture with macrophages at a 1:1 ratio in αMEM (L-glutamine, 0.25% FBS) for 18-20h. For the analysis of Stat3 and NF-κB activation, cocultures of MΦ and RM1(HA) were incubated for 5 and 20h as indicated. In specified experiments, MΦ were pre-treated for 1h with inhibitors of Stat3 activation, Stattic (#573099, Millipore; 12.5μM) or of NF-κB signaling, Bay-11-7082 (#196870, Millipore; 20μM) prior to coculturing with RM1(HA) cancer cells. In the case of Stattic, the culture media was replaced to remove the inhibitor prior to coculture.

Inflammation antibody array

Macrophages were cocultured with RM1(HA), PC3(HA), BMSC(HA), or MC4(HA) cells at a 1:1 ratio in αMEM (L-glutamine, 0.25% FBS). Supernatants were collected after 24h and analyzed using the mouse inflammation antibody array from RayBiotech, Inc. (#AAM-INF-1-8) following manufacturer's protocol. Protein collected from tumors was analyzed using the mouse inflammation antibody array from RayBiotech (400μg total protein/sample).

qRT-PCR

Total RNA was isolated from macrophages alone, macrophages cocultured with the following highly-apoptotic (HA) cells: RM1, PC3, BMSC, MC4, MPEC and BMC using the RNeasy® Mini Kit (Qiagen, #74104) per manufacturer's instructions. qPCR was performed using TaqMan gene expression master mix (Applied Biosystems, #4369016) and TaqMan probes: CXCL5 (Mm00436451_g1), CXCL1 (Mm04207460_m1), IL-6 (Mm00446190_m1), CCL5 (Mm01302427_m1) and GAPDH (Mm99999915_g1). Real time PCR was analyzed

on ABI PRISM 7700 (Applied Biosystems). Relative expression levels were calculated after normalization to GAPDH expression.

Plasmids and Virus Production

A minimal TATA-box promoter (Panomics) was introduced to a lentivirus-producing transfer vector construct (Addgene). This construct was further modified to generate a library of reporters, as described previously (1, 2). Each reporter contained a consensus binding sequence of a particular transcription factor in the enhancer region, driving expression of the firefly luciferase reporter gene. Consensus sequences were identified from available databases (e.g. TRANSFAC), commercial sources (e.g. Promega), and previous reports (3, 4).

Lentivirus was produced using established protocols (5). Human embryonic kidney (HEK) 293T cells (ATCC) were co-transfected with lentiviral packaging vectors and transfer vector constructs from the reporter library using jetPRIME (Polyplus-transfection). After 48h of incubation, supernatants were collected and viruses were concentrated using PEG-it (Systems Biosciences). Virus titers (>$5x10^8$ viral genomes) were measured using a Lentivirus qPCR Titer Kit (Applied Biological Materials (abm)).

Live imaging of TRanscriptional Activity CEll aRrays (TRACER)

Array setup was performed according to previous experiments with slight modifications (6). Macrophages were obtained by in vitro differentiation of primary murine bone marrow cells. Briefly, hind limbs of 6-12wk-old C57BL/6J mice were flushed to obtain a single cell suspension. Red blood cells were lysed and remaining cells were plated in suspension dishes containing RPMI-1640 (Life Technologies) supplemented with 10% FBS (Life Technologies), 1% penicillin/streptomycin (Life Technologies), and 20% L929 (a mouse cell line known to secrete M-CSF) conditioned media. Culture media was replaced after 3d. On d6, cells were collected using Versene (Life Technologies). Separate 1.5mL microcentrifuge tubes were filled with differentiated bone marrow-derived macrophages for batch viral infection. Lentiviral vectors sensitive for distinct transcription factor binding were introduced at a multiplicity of infection (MOI) of approximately 20 viral particles per cell. The suspension was seeded at 250,000 cells/mL in black 96-well plates (Corning). After incubation for 72h, media was replaced with αMEM supplemented with 0.5% FBS and 2mM D-luciferin (Perkin Elmer). Approximately 4h later, an equal volume of αMEM containing 500,000 cells/mL of apoptotic RM1 or MC4 cells were added. Treatment groups for each reporter were represented with n=4 measurements per plate. Following the addition

of apoptotic cells, bioluminescence measurements were acquired at 0, 2, 5, 8h using an In vivo Imaging System (Perkin Elmer).

ELISA

Tumors were mechanically dissociated and transferred to protein lysis buffer (Cell Signaling, #9803S) complemented with protease inhibitor cocktail (Thermo Scientific, #78410). CXCL1 and CXCL5 were quantitatively measured using RayBio® Mouse ELISA kits (RayBiotech, Inc. #ELM-KC and #ELM-LIX) using 400µg of protein per well. For in vitro analysis, supernatants were collected from cultures of MΦ alone, MΦ cocultured with RM(HA) cells, and MΦ cocultured with PC3(HA) cells. CXCL1 and CXCL5 concentrations were measured using RayBio® Mouse ELISA kits.

Human serum was collected from a cohort of 22 bone-metastatic prostate cancer patients enrolled in a clinical study at the University of Michigan Comprehensive Cancer Center (#XL184). Patients met the criteria of confirmed castrate-resistant prostate cancer metastatic to bone with multiple lesions (11 patients with >10, 10 patients with 3-10, and 1 patient with <3 lesions) and progressive disease marked by consecutively rising PSA levels (measured 1 week apart) or the emergence of >+2 new bone lesions. Patients received no prior chemotherapy for metastatic disease and no radiation therapy within 14d of the study, had no ongoing/active infection and no history of other malignant disease within the past 2yr. Serums were also collected from 40 patients (pre-treatment serum PSA≥20ng/mL and/or Gleason score of 8-10 and no evidence of distant or regional metastases) with high-risk localized disease prior to undergoing radical prostatectomy or prostate radiotherapy. Lastly, serums were collected from 20 normal (non-cancer) patients as controls. Human serum concentration levels of CXCL5, CXCL6 and IL-8 (CXCL8) were quantitatively measured using RayBio® Human ELISA Kits for ENA-78 (CXCL5; #ELH-ENA78), GCP-2 (CXCL6; #ELH-GCP2-1) and IL-8 (CXCL8; #ELH-IL8-1).

Western Blot

Cells were washed with PBS and lysed with protein lysis buffer (#9803, Cell Signaling Technology) supplemented with protease inhibitor cocktail (Thermo Scientific, #78410). Electrophoresis was performed with 4-20% Tris-Glycine gels (Invitrogen, 20µg of protein/well). Proteins were transferred to PVDF membranes (Bio-Rad), blocked with 5% milk in 1xTBST and incubated for 16h at 4^{o}C in 5% BSA in 1xTBST with the following antibodies: Caspase-9 (C9) (#9508), cleaved Caspase-3 (Asp175) (5A1E) (#9664), Phospho(P)-NF-

κB(p65) (Ser536) (93H1) (#3033), Phospho(P)-Stat3 (Tyr705) (#9131), and NF-κB2(p100/p52) (#4882), (Cell Signaling). Membranes were then washed and incubated with the recommended secondary antibodies (Cell Signaling), washed, developed using chemiluminescence substrate (#34075, Thermo Scientific) and imaged on film (Figure 2A), or via the ChemiDoc™ Touch Imaging System (Bio-Rad) (Figure 3). Protein bands were quantified and normalized using the Image Lab™ Software (Bio-Rad).

Flow Cytometry

Tumors were mechanically dissociated followed by digestion in complete RPMI-1640 media supplemented with type I collagenase (5mg/mL; Sigma-Aldrich) and 0.5% FBS. Red blood cells were lysed using ACK buffer (Gibco, #A10492-01) according to manufacturer's instructions. Viable cells were counted and $1x10^6$ were incubated in FACS staining buffer containing Fc Block (BD Pharmingen, #553142) and combinations of antibodies and/or isotype controls. Antibodies from Abcam: FITC-Ly6B (7/4) (#ab53453) and APC-F4/80 (Cl: A3-1) (#ab105080). Antibodies from BioLegend: FITC-CD68 (FA-11) (#137006), FITC-CD86 (GL-1) (#105006), FITC-CD206 (C068C2) (#141704), FITC-Ly6C (HK1.4) (#128006), FITC-Gr-1 (RB6-8C5) (#108406), FITC-Ly6G (1A8) (#127605), PB-F4/80 (BM8) (#123124), (APC-CD206 (C068C2) (#141708), APC-CD86 (GL-1) (#105012), and APC-CD11b (M1/70) (#101212). Matched isotype controls were used for all antibodies. Cells were analyzed by flow cytometry on the BD FACSAria™ III.

Macrophage Coculture with Apoptosis-Inducible Cancer Cells

Macrophages ($1x10^6$) were cocultured with RM1-iC9 cells (1:1 ratio), incubated with AP20187 (B/B homodimerizer 500nM, Clontech, #635060, a ligand that induces iCaspase-9 dimerization and apoptosis in RM1-iC9) and/or Emetine (0.3μM) (reported NF-κB inhibitor shown to inhibit IkBα phosphorylation; Sigma, #E2375 (7)), Stattic (12.5μM) or Bay-11-7082 (20μM) (as described above) for 18-20h. Cells were then analyzed by flow cytometry using the Amnis® Imaging flow cytometer. For in vitro flow cytometry, $1x10^6$ cells were suspended in flow buffer (PBS containing 0.3% BSA) and incubated with combinations of Rat anti Mouse Ly-6B.2 Alloantigen: FITC antibody (7/4) (Bio-Rad, #MCA771F), PE-P-Stat3 (Tyr 705) (#8119, Cell Signaling), PE-P-p65 (SER536) (#5733, Cell Signaling) and APC-F4/80 (Cl: A3-1) (#ab105080) antibodies and/or matched isotype controls.

Immunohistochemistry staining and quantification

Tumors were collected and fixed in 10% formalin and embedded in paraffin blocks. Immunofluorescence staining was performed by Opal™ 4-color fIHC Kit (PerkinElmer, #NEL794001KT), according to manufacturer's instructions using the Rat monoclonal antibody F4/80 (CI: A3-1) (1:600, Abcam, #ab6640) and monoclonal rat anti-mouse Ly-6B.2 alloantigen antibody (7/4) (1:250, Bio-Rad, #MCA771G). Confocal microscopy images were obtained using Leica SP5 inverted confocal microscope and Leica software (Leica Microsystems). Positively stained cells were quantified by counting two different regions inside each tumor (*n*=8/group) at 10x magnification per field of view (FOV).

Vossicle (vertebral body) subcutaneous RM1-iC9 tumors

The vossicle model, which provides an osseous scaffold for tumor growth in a bone microenvironment, has been previously described (8-10). Briefly, 7d-old postpartum C57BL/6J wild type (WT) or $CXCL5^{-/-}$ donor mice were sacrificed and lumbar vertebrae were carefully isolated. After washing with PBS, every two lumbar vertebral disks were dissected to obtain vossicles. RM1-iC9 ($2x10^3$) tumor cells were injected into each vossicle and immediately implanted in a subcutaneous pouch on the right side of the back of WT or $CXCL5^{-/-}$ anesthetized recipient mice. Wounds were closed with surgical clips and animals were monitored daily. Wild type (WT) mice were randomized and assigned to treatments groups (vehicle (VEH) or AP20187 (AP)). At d7 and 11 mice were treated with VEH or AP (5mg/kg) by intraperitoneal injection to induce apoptosis in RM1-iC9 cells. Tumors were measured daily by caliper. When the study endpoint was reached (approximately $1.5cm^3$ tumor volume or 13d after implantation), tumors were dissected, weighed and processed for posterior analyses.

Intratibial injection model

Apoptosis-inducible RM1-iC9 murine prostate cancer cells ($2x10^3$) or RM1-iC9-GFP (RM1-iC9 cells transduced cells with GFP-reporter lentiviral construct (Lenti-GFP, University of Michigan Vector Core)) were inoculated via intratibial injection in the left tibias of C57BL/6J mice and under anesthesia as previously described (10). The right tibias were not injected and used as non-tumor controls. Two experimental approaches were performed: 1) To understand the early effects of AP in the efferocytosis of apoptotic cancer cells, C57BL/6J mice were injected with RM1-iC9-GFP and at d5, mice were treated with vehicle (VEH) or AP20187 (AP, 5mg/kg) and the treatment extended for 5h before the end point. Mice were sacrificed and both tibias (tumor-injected and control) were dissected, bone marrow was flushed with flow buffer and red blood cells were lysed

using ACK lysing buffer for early cell analyses by flow cytometry using the APC-labeled CD11b or F4/80 antibodies or their matched isotypes (APC-IgG) controls. 2) To determine changes in the bones and advanced tumor progression, RM1-iC9 were injected and then treated with VEH or AP at d6 and 8. Mice were sacrificed at d9 and both tibias were immediately fixed in 4% paraformaldehyde for 24h and maintained in 70% ethanol for μCT analyses. Then tibias were decalcified in 10% EDTA (21d) at 4°C and paraffin-embedded for histological analyses. One left tibia from VEH group did not form tumor and was excluded from the analyses. Tibial sections were stained with tartrate resistant acid phosphatase (TRAP) (Sigma-Aldrich #387A) per manufacturer's instructions. Images were taken at 10x and stitched together to construct whole bone images. For osteoclast quantification the ROIs began 200μm distal to the proximal growth plate, extended 1200μm distally and spans 50μm from endocortical surface. Within these ROIs the osteoclast surface (Oc.S), bone surface (BS) and osteoclast number (N.Oc) were quantified inside the tumor areas using the OsteoMeasure software (OsteoMetrics Inc) according to the standard protocols (11). Histological tumor areas in H&E sections were delineated utilizing the ImageJ program for total tumor area determination relative to total bone area (Tm.Ar/T.Ar).

For the intratibial inoculation in wild type (WT) and CXCL5$^{-/-}$ mice a similar approach was used except that both groups were treated with AP at d6 and 8 post-injection to maximize inflammation and CXCL5 expression in the bone microenvironment. One left tibia from CXCL5$^{-/-}$ mice did not form tumor and was excluded from the analyses.

μCT imaging

Fixed tibias were scanned by μCT (Scanco μCT-100) at a 12mm voxel size and according to established guidelines as previously described (10, 12). Briefly, trabecular bone parameters were measured over 50 slices extending from 15 slices distal to the growth plate, while the cortical bone was measured over 30 slices at 60% of the bone length distal to the tibia-fibular junction (TFJ) using a 28% threshold. The total bone volume and total volume were measured from proximal to distal TFJ.

Human mononuclear cell isolation

Human peripheral blood mononuclear cells (PBMCs) were isolated under an Institutional Review Board-approved protocol (#HUM00052405) from 7.5mL of venous blood collected in EDTA-coated vacutainer tubes (Becton-Dickinson). Samples were collected at the University of Michigan Comprehensive Cancer Center from

patients with prostate cancer bone metastases as well as from healthy donors without any cancer history. Ficoll-Hypaque (GE Healthcare) density gradient centrifugation was performed, and the buffy coat was used immediately for FACS analysis to determine monocyte profiles using markers CD14 (3G8), CD16 (M5E2), and CD68 (Y1/82A) (Biolegend) (13). Efferocytosis was measured in a subset of samples using phosphatidylserine (PS) coated apoptotic mimicry beads fluorescently labeled (Bangs Laboratories) as bait and added at a 1:3 ratio for 1 hour. Cells were then washed and stained to detect $CD14^+$ cells (BioLegend). After incubation, cells were washed and subsequently fixed with 1% formaldehyde, then washed twice and evaluated using FACS analyses (BD FACSAria™ III and FlowJo v10). Results are expressed as percentage of cells that were positive for both CD14 (APC) and bead ingestion (PE).

Supplemental References:

1. Weiss MS, Penalver Bernabe B, Shin S, Asztalos S, Dubbury SJ, Mui MD, Bellis AD, Bluver D, Tonetti DA, Saez-Rodriguez J, et al. Dynamic transcription factor activity and networks during ErbB2 breast oncogenesis and targeted therapy. *Integr Biol.* 2014;6(12):1170-82.
2. Siletz A, Schnabel M, Kniazeva E, Schumacher AJ, Shin S, Jeruss JS, and Shea LD. Dynamic transcription factor networks in epithelial-mesenchymal transition in breast cancer models. *PLoS One.* 2013;8(4):e57180.
3. Romanov S, Medvedev A, Gambarian M, Poltoratskaya N, Moeser M, Medvedeva L, Gambarian M, Diatchenko L, and Makarov S. Homogeneous reporter system enables quantitative functional assessment of multiple transcription factors. *Nat Methods.* 2008;5(3):253-60.
4. Weiss MS, Bernabe BP, Shikanov A, Bluver DA, Mui MD, Shin S, Broadbelt LJ, and Shea LD. The impact of adhesion peptides within hydrogels on the phenotype and signaling of normal and cancerous mammary epithelial cells. *Biomaterials.* 2012;33(13):3548-59.
5. Boehler RM, Kuo R, Shin S, Goodman AG, Pilecki MA, Gower RM, Leonard JN, and Shea LD. Lentivirus delivery of IL-10 to promote and sustain macrophage polarization towards an anti-inflammatory phenotype. *Biotechnol and Bioeng.* 2014;111(6):1210-21.
6. Aguado BA, Wu JJ, Azarin SM, Nanavati D, Rao SS, Bushnell GG, Medicherla CB, and Shea LD. Secretome identification of immune cell factors mediating metastatic cell homing. *Sci Rep..* 2015;5:17566.
7. Miller SC, Huang R, Sakamuru S, Shukla SJ, Attene-Ramos MS, Shinn P, Van Leer D, Leister W, Austin CP, and Xia M. Identification of known drugs that act as inhibitors of NF-kappaB signaling and their mechanism of action. *Biochem Pharmacol.* 2010;79(9):1272-80.
8. Jung Y, Shiozawa Y, Wang J, McGregor N, Dai J, Park SI, Berry JE, Havens AM, Joseph J, Kim JK, et al. Prevalence of prostate cancer metastases after intravenous inoculation provides clues into the molecular basis of dormancy in the bone marrow microenvironment. *Neoplasia.* 2012;14(5):429-39.
9. Park SI, Kim SJ, McCauley LK, and Gallick GE. Pre-clinical mouse models of human prostate cancer and their utility in drug discovery. *Curr Protoc Pharmacol.* 2010;Chapter 14(Unit 14 5).
10. Soki FN, Cho SW, Kim YW, Jones JD, Park SI, Koh AJ, Entezami P, Daignault-Newton S, Pienta KJ, Roca H, et al. Bone marrow macrophages support prostate cancer growth in bone. *Oncotarget.* 2015;6(34):35782-96.
11. Dempster DW, Compston JE, Drezner MK, Glorieux FH, Kanis JA, Malluche H, Meunier PJ, Ott SM, Recker RR, and Parfitt AM. Standardized nomenclature, symbols, and units for bone histomorphometry: a 2012 update of the report of the ASBMR Histomorphometry Nomenclature Committee. *J Bone Miner Res.* 2013;28(1):2-17.

12. Bouxsein ML, Boyd SK, Christiansen BA, Guldberg RE, Jepsen KJ, and Muller R. Guidelines for assessment of bone microstructure in rodents using micro-computed tomography. *J Bone Miner Res.* 2010;25(7):1468-86.
13. Cros J, Cagnard N, Woollard K, Patey N, Zhang SY, Senechal B, Puel A, Biswas SK, Moshous D, Picard C, et al. Human CD14dim monocytes patrol and sense nucleic acids and viruses via TLR7 and TLR8 receptors. *Immunity.* 2010;33(3):375-86.

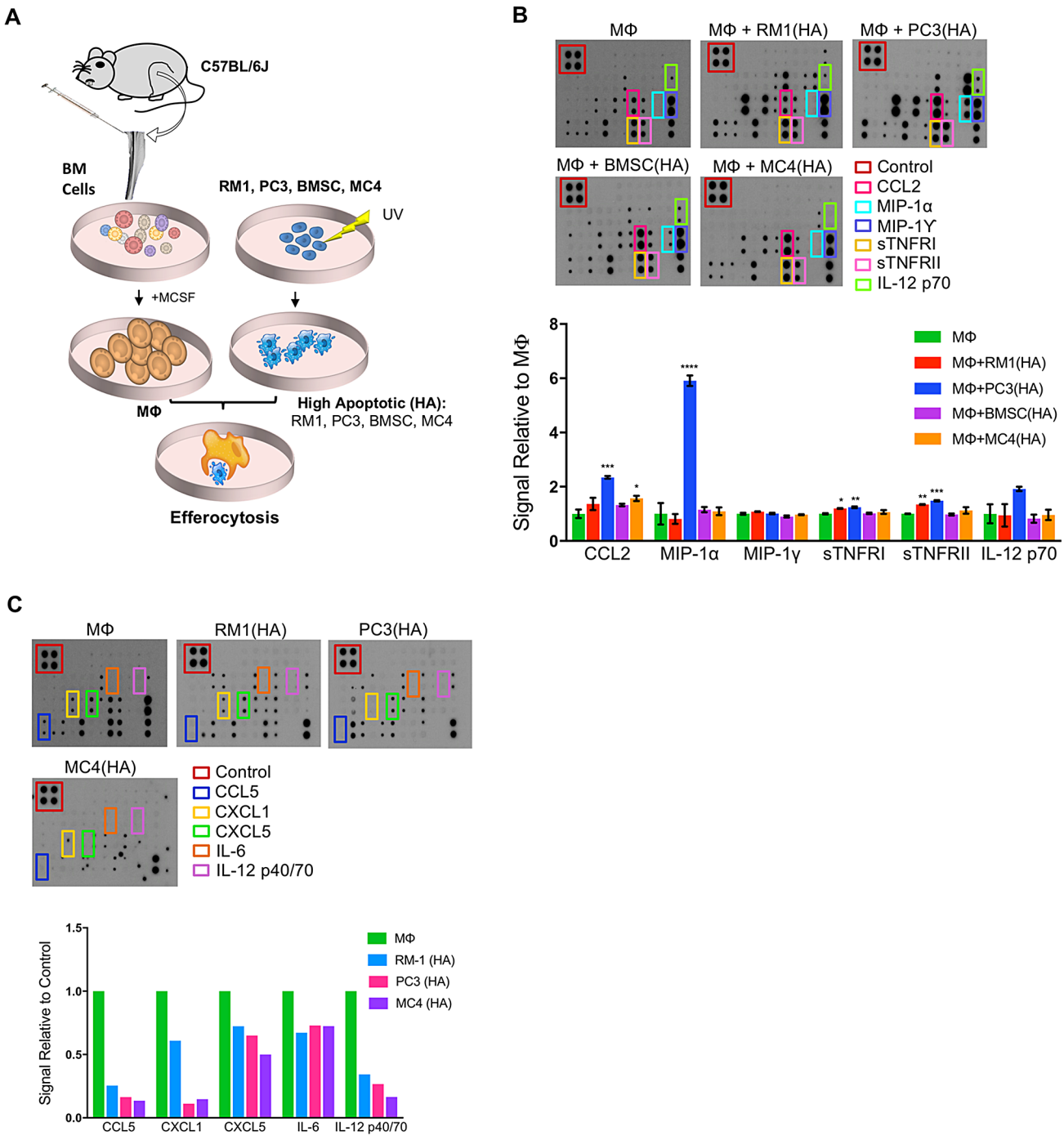

Figure S1: Analysis of cytokines in cocultures of macrophages and highly-apoptotic cells (HA) (related to Figure 1). A: Experimental design of bone marrow-derived macrophages (MΦ) cocultured with apoptotic cells to induce efferocytosis. **B:** Supernatants were collected from MΦ alone or cocultured with RM1(HA), PC3(HA), BMSC(HA), or MC4(HA) for 18h and efferocytosis-induced cytokines were analyzed and quantified via murine inflammatory cytokine array (also described in Figure 1). Data are mean ± S.E, *p<0.05, **p<0.01, ***p<0.001, ****p<0.0001 vs. macrophage alone, *n*=3/cell type; (one-way ANOVA). **C:** Cytokine expression in apoptotic cells alone compared to MΦ alone. Data are normalized to MΦ and are presented as mean, *n*=2/cell type.

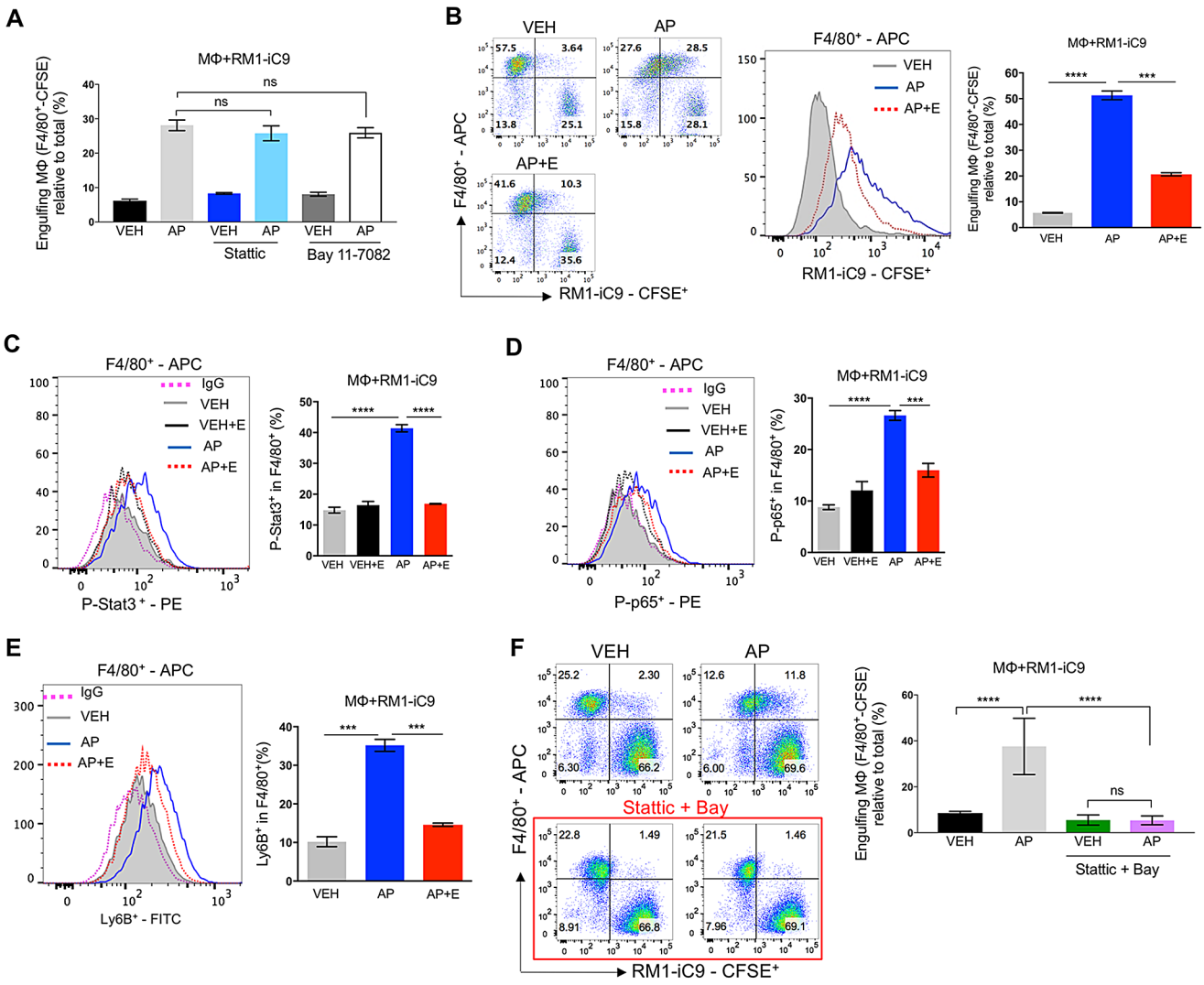

Figure S2. **Signaling activation of Stat3 and NF-κB(p65) in macrophages efferocytosing apoptosis-induced RM1-iC9 cells (related to Figure 3). A**: Flow cytometric analysis of MΦ-efferocytosis of RM1-iC9 ($CFSE^+$) treated with VEH or AP in cocultures pre-treated with Stattic (12.5 μM), or Bay-11-7082 (20 μM). MΦs were stained with F4/80-APC antibody. The engulfing $F4/80^+$-MΦs were determined as the double positive $APC^+/CFSE^+$ population. Graph depicts percentage of $F4/80^+/CFSE^+$ relative to total $F4/80^+$ cells. **B**: Flow analysis showed MΦ-efferocytosis of RM1-iC9 treated with VEH, AP, or AP + E (NF-κB inhibitor Emetine, 0.3 μM). The histograms depict the $CFSE^+$ populations in the total APC^+ ($F4/80^+$) cells for each group. Graph shows engulfing APC^+ $F4/80^+/CFSE^+$ cells relative to total APC^+. **C-D:** Analysis of phosphorylation of Stat3 **(C)** and NF-κB (RelA/p65) **(D)** in cocultures of MΦs and RM1-iC9. Cells were stained using F4/80-APC, P-Stat3-PE and P-p65-PE antibodies as indicated. The histograms depict the PE^+ populations in the total APC^+($F4/80^+$) population for each group. The graph shows PE^+/APC^+ relative to total APC^+ cells for each group. **E**: Flow cytometric analysis of $Ly6B^+$(FITC) and $F4/80^+$(APC) in cocultures of MΦ and RM1-iC9 cells treated with VEH, AP and Emetine (E), as indicated. The histograms depict the $FITC^+$ cells in the total APC^+ population for each group. The percentages in the graph ($Ly6B^+$ in F4/80) are relative to total $F4/80^+$ cells: $(FITC^+/APC^+)$/(total APC^+ cells). The histograms corresponding to IgG-isotype controls are shown in C-E. **F**: Representative flow plots of $F4/80^+$ MΦs engulfing RM1-iC9 ($CFSE^+$) treated with VEH or AP. MΦs were pretreated for 1h with VEH or a combination of Stattic and Bay 11-7082. Data are presented as mean ± S.E., *n*=3/group (except **F** *n*=6/group); ***p<0.001, ****p<0.0001, n.s-not significant (One way ANOVA).

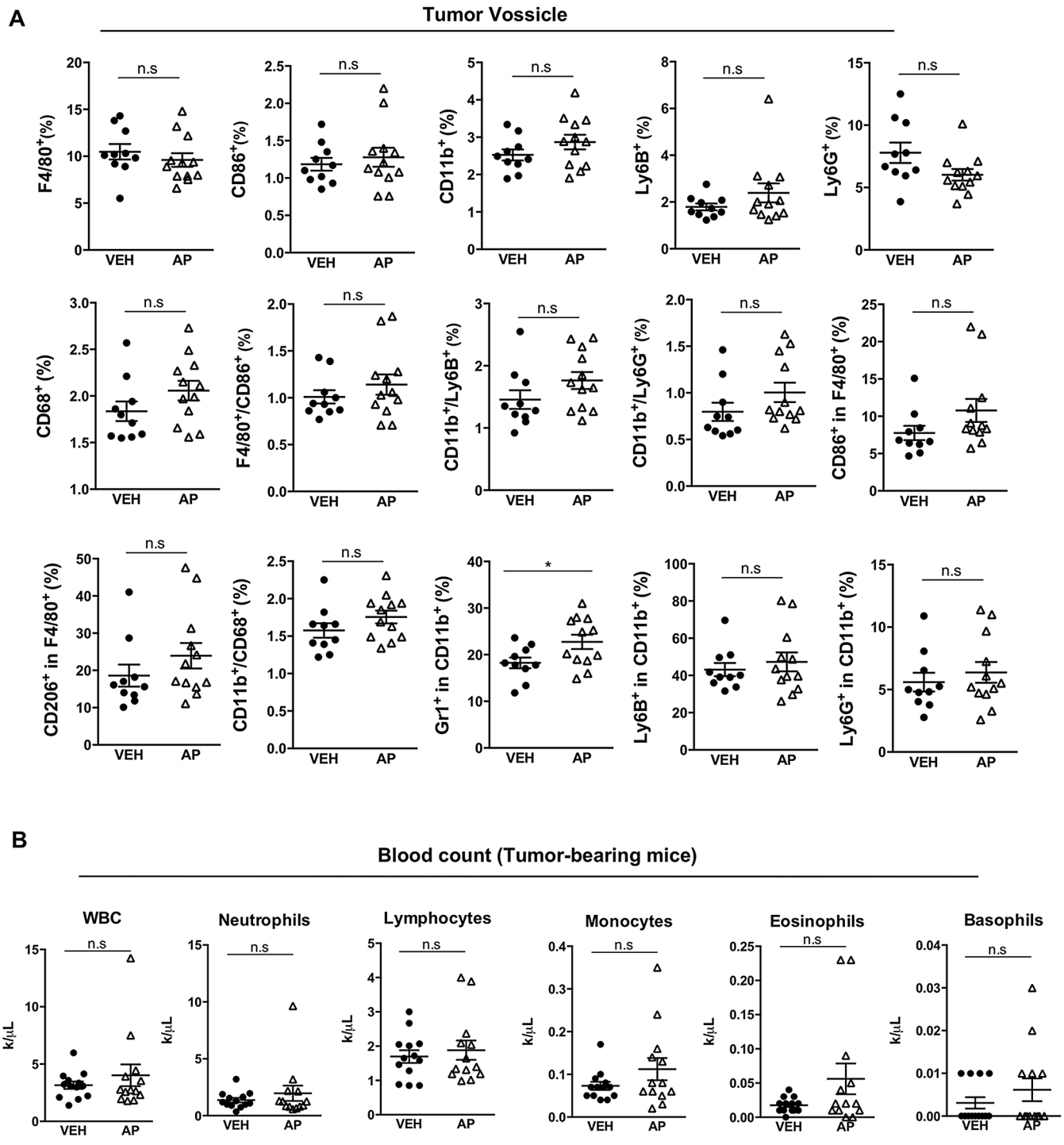

Figure S3: Flow cytometric and blood count analysis of tumor-vossicle cell populations (related to Figure 5). Vossicles from C57BL/6 donor mice (7d males) were inoculated with RM1-iC9 cells, and subcutaneously implanted in C57BL/6 male recipient mice (7wk). Mice were randomly divided into two groups treated with vehicle (VEH) or AP20187 (AP) to induce apoptosis in RM1-iC9 cells and subsequent efferocytosis. **A:** Thirteen days after vossicle implantation, a quantitative analysis of tumor cell population was performed by flow cytometry in VEH (*n*=10) and AP (*n*=12) groups. Gates were established according to IgG-isotype controls for each antibody. **B:** Blood count analysis of mice bearing tumor-vossicles at the time of sacrifice. Data are mean ± S.E., *n*=13/group; *p<0.05, n.s-not significant (two-tailed Student's *t*-test).

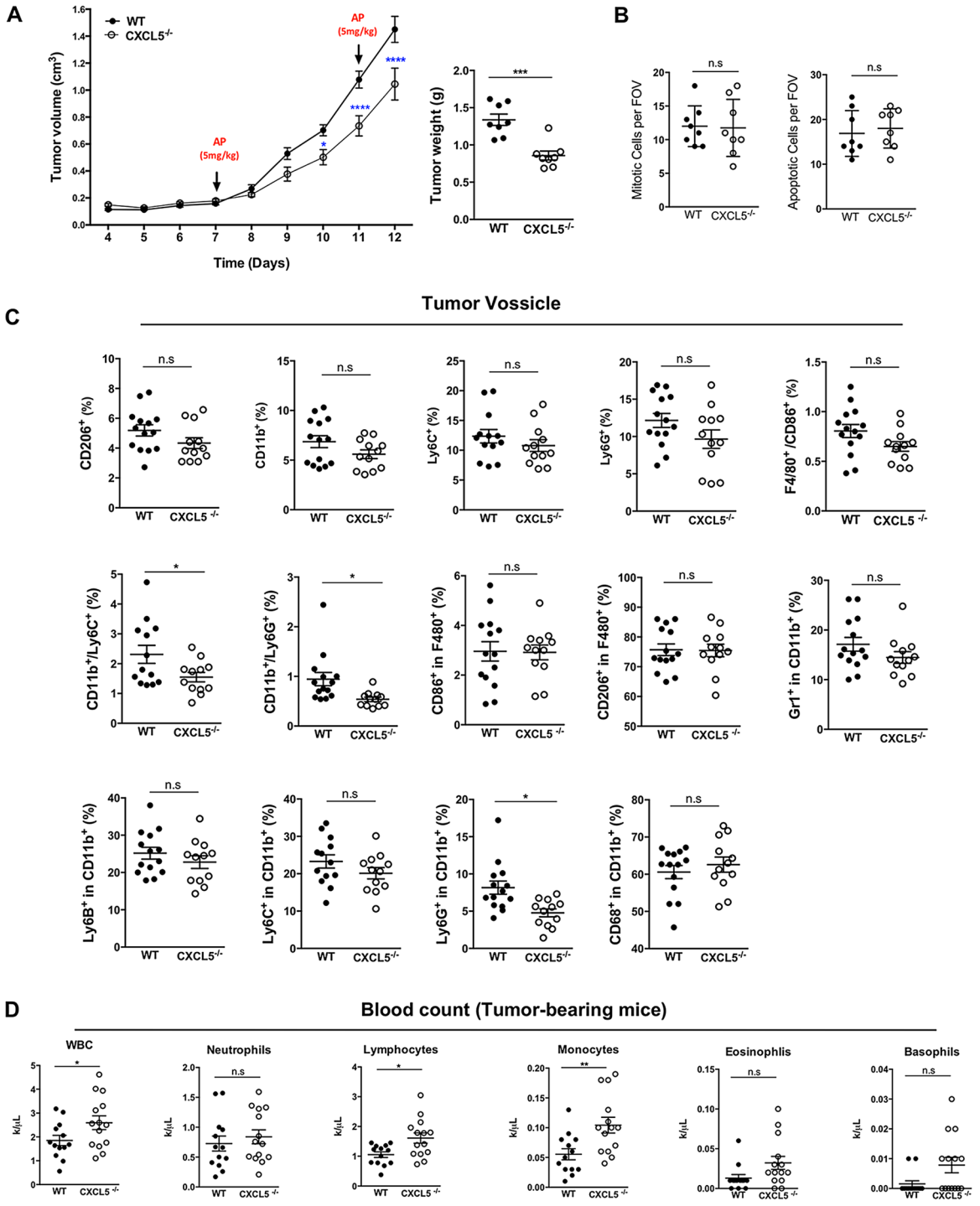

Figure S4: **CXCL5$^{-/-}$ mice hindered prostate cancer growth in the bone-vossicle model (related to Figure 6).** WT and CXCL5$^{-/-}$ recipient mice (7wk males) were implanted subcutaneously with RM1-iC9 inoculated vossicles isolated from WT or CXCL5$^{-/-}$ donor mice (7d males) respectively (one vossicle implanted per mouse). Recipient mice from both groups were treated with AP at d7 and 11 to induce cancer-cell death and efferocytosis. **A:** Depicts tumor growth similar to the experiment represented in Figure 6A. Tumor-vossicle volume was measured daily starting at d4 until sacrifice. Tumor weight was quantified upon sacrifice. Data are mean ± S.E., *p<0.05, ****p<0.0001 (two-way ANOVA) vs. wild-type controls; *n*=8/group. Tumor weight was analyzed with two-tailed Student's *t* test ***p<0.001. **B:** Mitotic and apoptotic cells were quantified inside non-necrotic tumor areas (4 fields at 20X per tumor-vossicle sample), *n*=8/group. **C:** Flow cytometric analysis of tumor-vossicle cell populations from WT (*n*=14) and CXCL5$^{-/-}$ (*n*=12) mice. **D:** Complete blood count (CBC) analysis of tumor-bearing mice; WT (*n*=13) and CXCL5$^{-/-}$ (*n*=14) mice. Data in **B-D** are mean ± S.E, *p<0.05, **p<0.01, n.s-not significant (two-tailed Student's *t*-test).

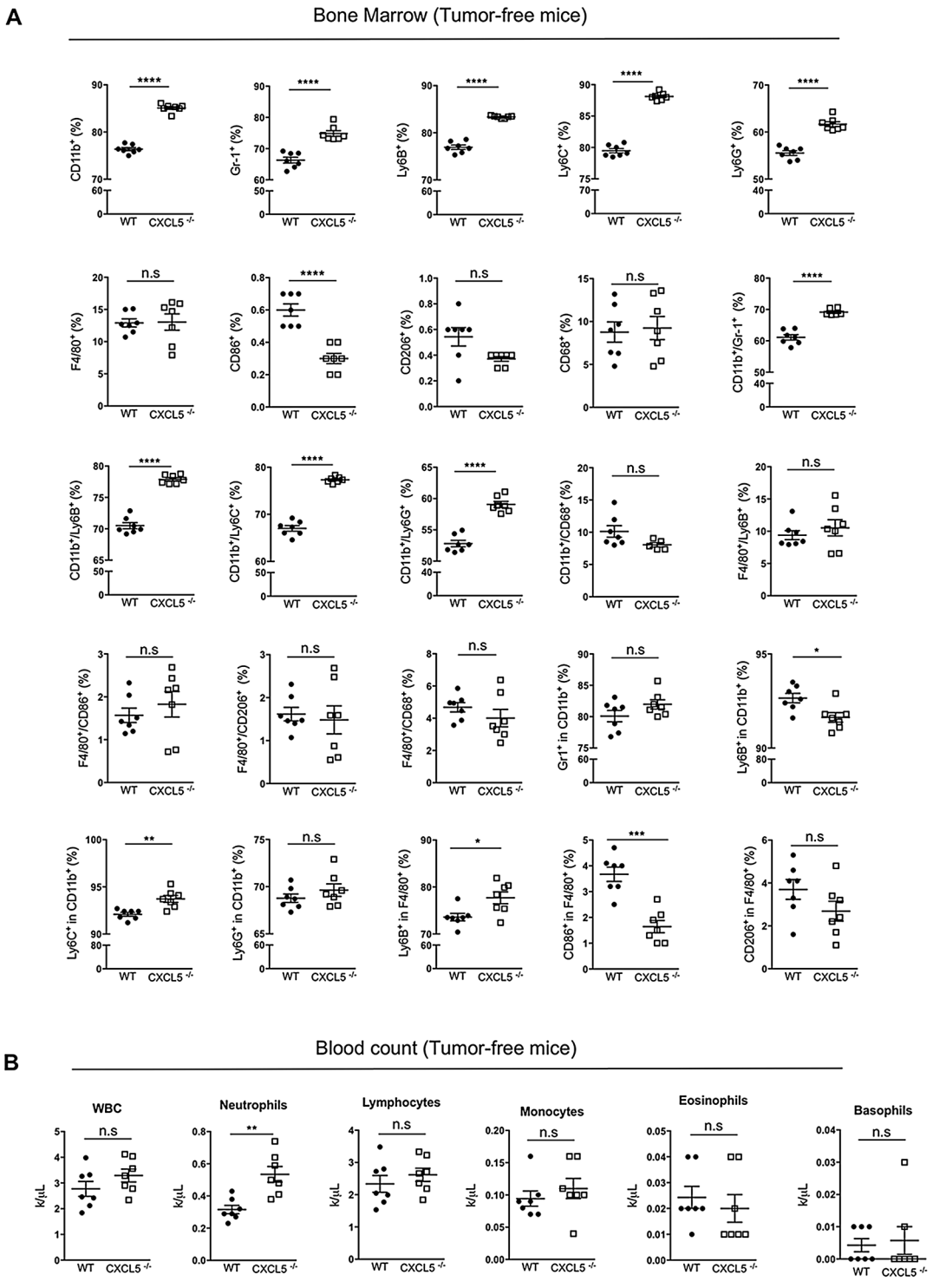

Figure S5: **Bone marrow cell populations from WT and CXCL5$^{-/-}$ tumor-free mice were analyzed by flow cytometry (related to Figure 8). A:** Specified bone marrow cell populations from tumor-free WT and CXCL5$^{-/-}$ (*n*=7/group). **B:** Blood was collected from tumor-free WT and CXCL5$^{-/-}$ mice and analyzed by CBC, *n*=7/group. Data are mean ± S.E., *p<0.05, **p<0.01, ***p<0.001, ****p<0.0001, n.s-not significant (two-tailed Student's *t*-test).

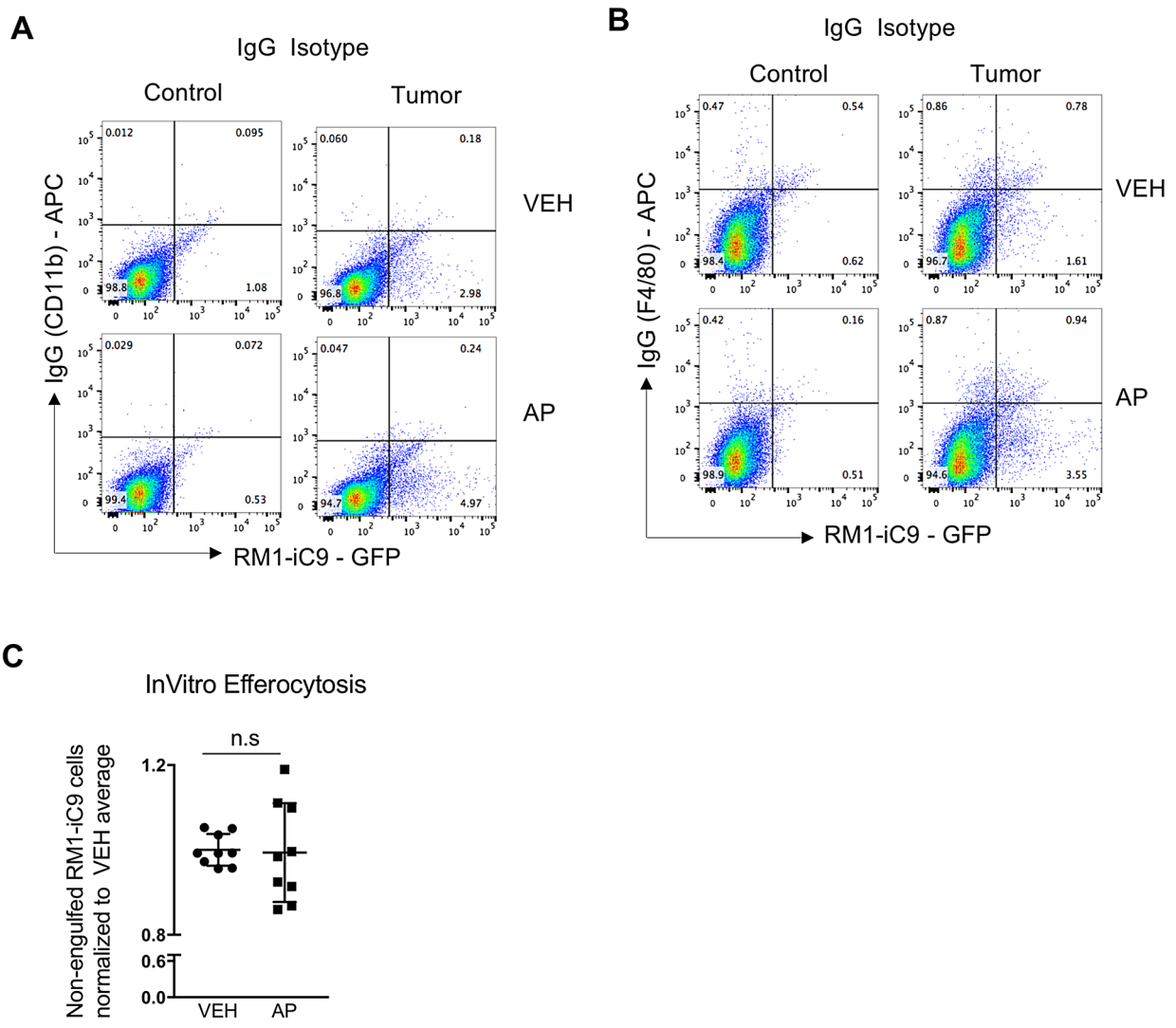

Figure S6. **Engulfment of apoptosis-inducible RM1-iC9 prostate cancer cells (related to Figure 9)**. Representative flow cytometry plots of bone marrow cells corresponding to Vehicle control (VEH) and AP-treated mice isolated from tumor-inoculated and contralateral (non-tumor) control tibias using the APC-labeled IgG-isotype antibodies (as indicated) to determine gates used in Figure 9. **A:** Flow cytometry plots obtained with the IgG (CD11b)-APC antibody (denotes the APC-labeled Isotype control corresponding to the CD11b antibody). **B:** Flow cytometry plots obtained with the IgG (F4/80)-APC antibody (denotes the APC-labeled Isotype control corresponding to the F4/80 antibody). **C:** Non-engulfed cancer cells ($CFSE^{+}/F4/80^{-}$) analyzed in vitro from cocultures of MΦs and CFSE-labeled RM1-iC9. Flow cytometry results were calculated from 3 independent experiments (*n*=3 mice/experiment; total *n*=9) and represented in the graph after normalization to the VEH group average. Data are mean ± S.E., n.s-not significant (two-tailed Student's *t*-test).

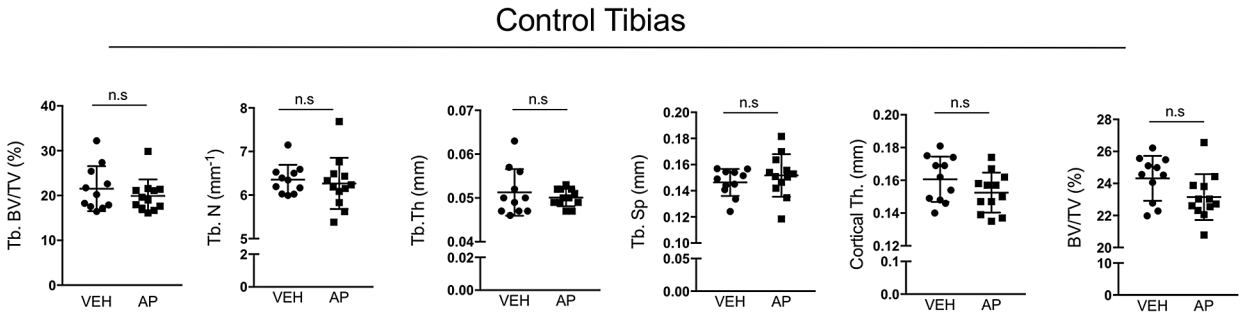

Figure S7. AP-treatment analysis of bone parameters in contralateral (non-tumor) control tibias (related to Figure 10). Bone parameters were quantified by μCT for VEH (*n*=11) and AP (*n*=12) contralateral tibias. Trabecular bone volume relative total volume (Tb BV/TV), trabecular number (Tb.N), trabecular thickness (Tb.Th), trabecular spacing (Tb.Sp), cortical thickness (cortical Th) and total bone volume relative to total volume (BV/TV) were quantified. Data are mean ± S.E, n.s-not significant (two-tailed Student's *t*-test).

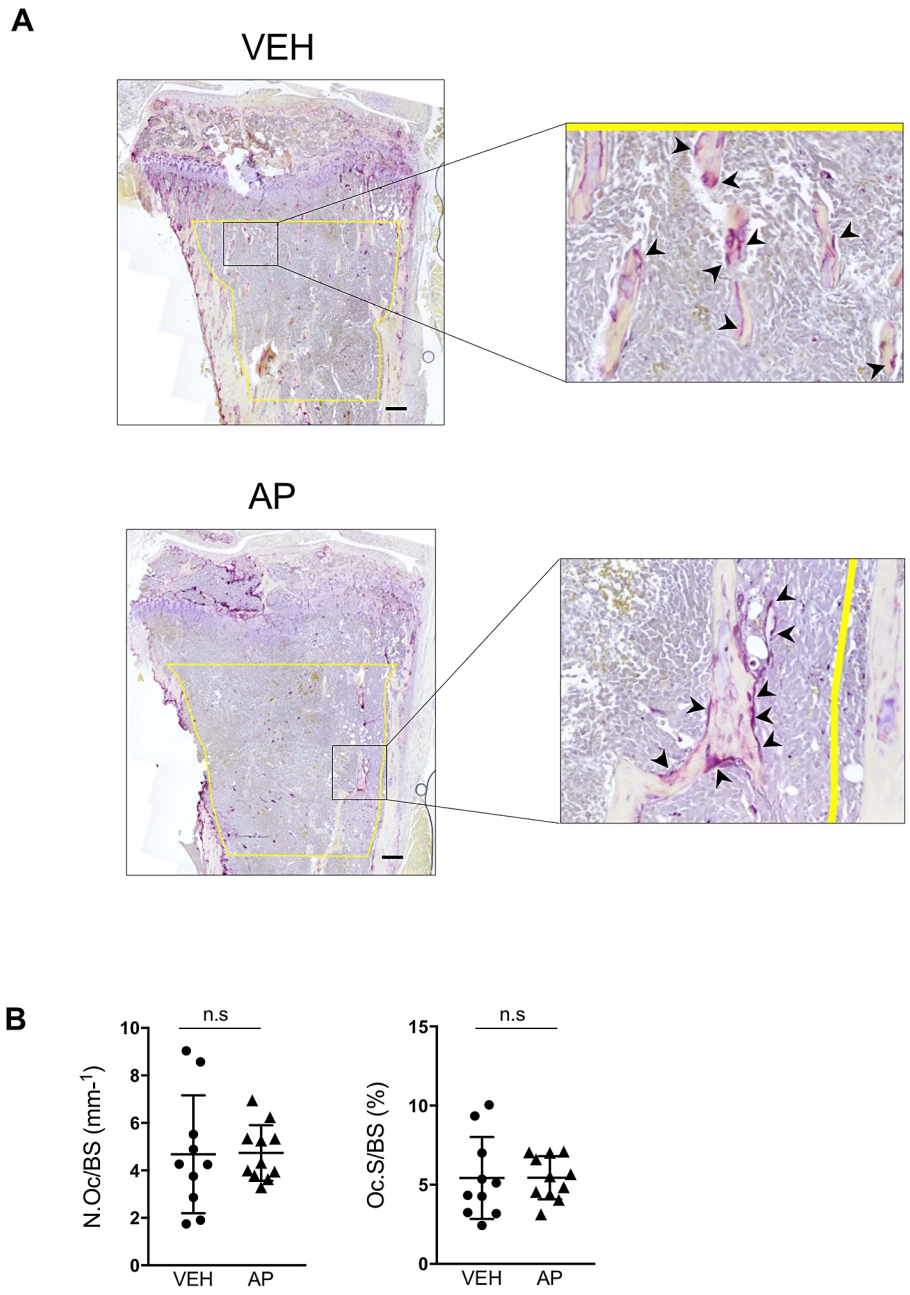

Figure S8. TRAP5b analysis in Intratibial tumor model showing no difference with AP-treatment (related to Figure 10). A: Representative images of TRAP osteoclast staining (ROI outlined with yellow line). Some TRAP^{+}-osteoclasts are shown attached to bone in the amplified image (right) (scale 400µm) **B:** TRAP^{+}-osteoclast surface per bone surface (Oc.S/BS) and osteoclast numbers per bone surface (N.Oc/B.S) were quantified by histomorphometric analyses inside the tumor area; VEH (*n*=10) and AP (*n*=11). Data are mean ± S.E, n.s-not significant (two-tailed Student's *t*-test).

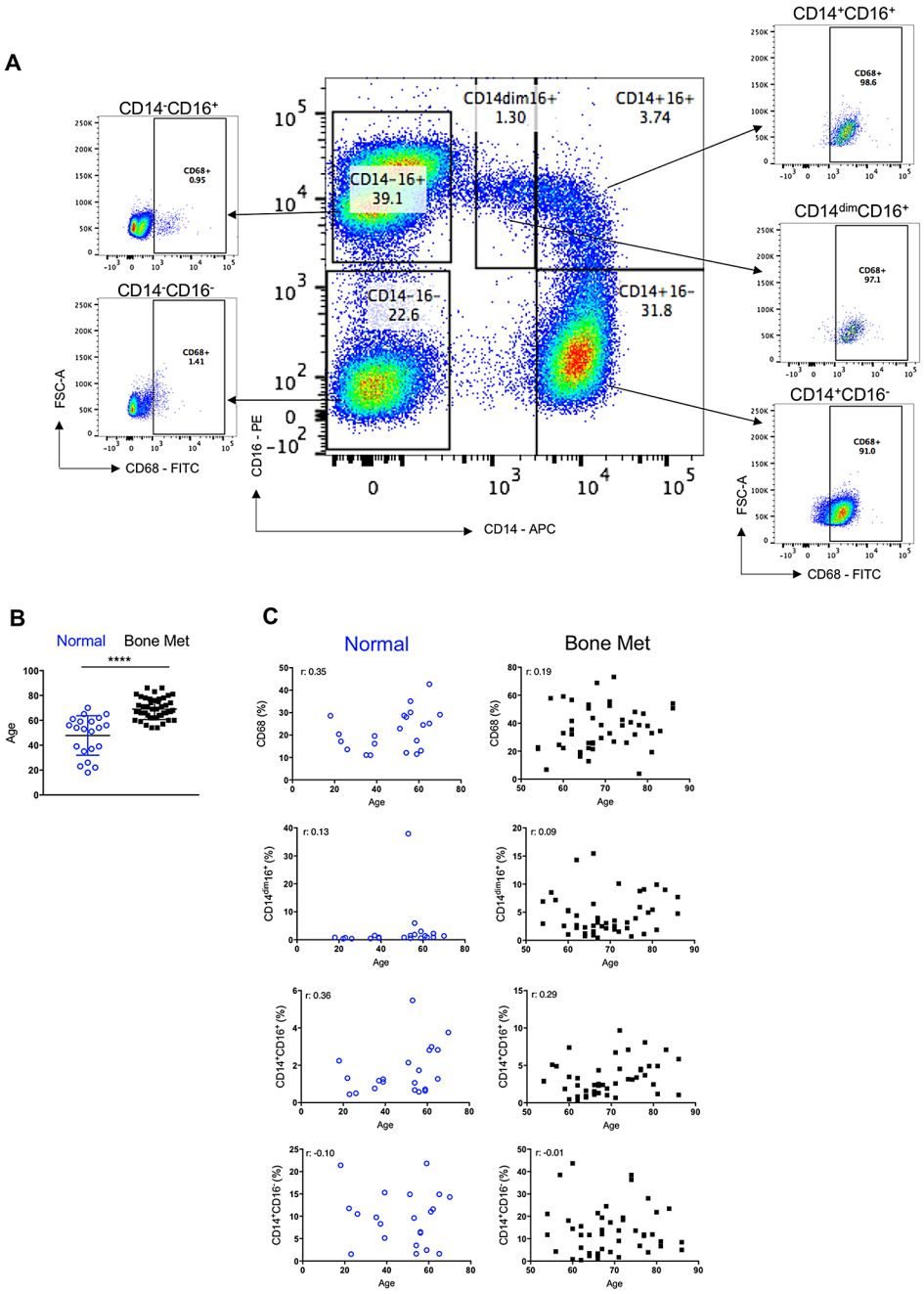

Figure S9: **CD68 staining in peripheral mononuclear cell populations showed expression in CD14$^+$ cells (related to Figure 12). A:** Representative sample of a bone-metastatic patient. Percentages of CD68$^+$ cells are shown for the different gated monocyte subpopulations (CD14$^-$16$^-$, CD14$^-$16$^+$, CD14^{dim}16$^+$, CD14$^+$16$^+$ and CD14$^+$16$^-$). **B:** Age distribution in the patient blood samples (Normal and Bone Met) corresponding to the experiments described in Figure 12 A-B. Data are mean ± S.E, ****p<0.0001 (two-tailed Student's *t*-test). **C:** Plots showing the distribution of the different blood populations (expressed as percentages relative to total peripheral blood mononuclear cells) in relation to patient age of the samples. No significant correlation was found in percentages of different populations relative to the age of patients within each group of Normal and Bone Met (Pearson correlation analysis, p>0.05).

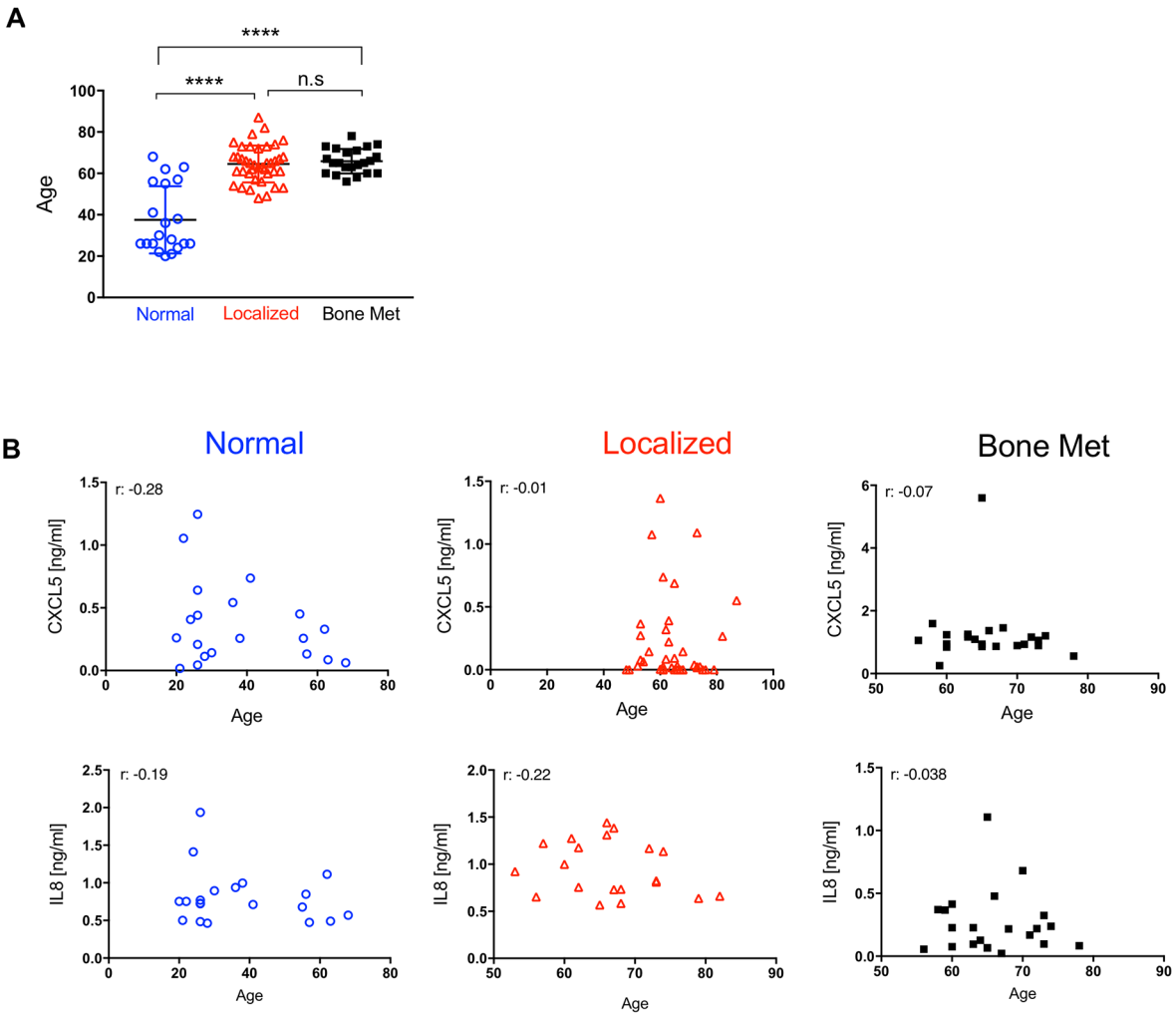

Figure S10: **Age distribution in the patients of Normal, Localized and Bone Met serum samples (related to Figure 12 D-F). A:** Plots of patients' ages in the different groups. No differences were found between Localized and Bone Met ages; however, ages of Normal controls were significantly lower. Data are mean ± S.E, ****p<0.0001 (two-tailed Student's *t*-test). **B:** Distribution of the cytokine values determined by ELISA relative to the age of patients in the different groups. No significant correlation was found in the cytokine values relative to the age of patients within each group of Normal, Localized and Bone Met (Pearson correlation analysis, p>0.05).

Supplemental Table 1. Clinicopathological Parameters of Prostate Cancer Skeletal Metastasis Patients used to characterize the circulating monocytes*.

Age	Castrate Resistant	Gleason	PSA [ng/ml]
50-64 (N=15)	Yes (N=28)	6 (N=2)	<20 (N=17)
65-74 (N=19)	No (N=2)	7 (N=12)	≥20 (N=18)
75+ (N=13)		8 (N=2)	
		9 (N=14)	
		10 (N=2)	

* This information is incomplete for some patients used in the experiment

Supplemental Table 2. Characteristics of Bone Met patients used to determine the serum level of pro-inflammatory cytokines.

Age	Number of Bone Lesions	Prostatectomy
50-60 (n=5)	<3 (n=1)	Yes (n=7)
61-69 (n=8)	3-10 (n=10)	No (n=14)
70+ (n=7)	>10 (n=11)	

Full unedited blots for Figure 2A
From Top to Bottom

Blot 1 (Caspase-9 Ab)

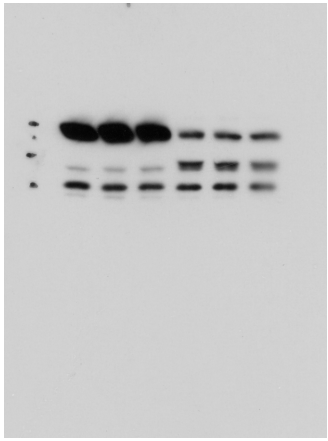

Blot 2 (Cleaved Caspase-3 Ab)

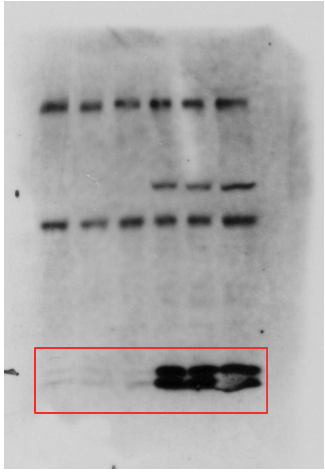

Full unedited blots and gel for Figure 3A
From Top to Bottom

Blot 1 (P-p65 Ab)

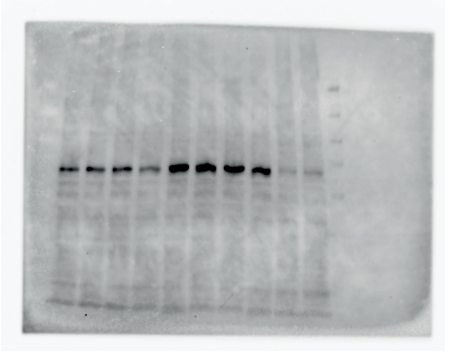

Gel (Total Protein)

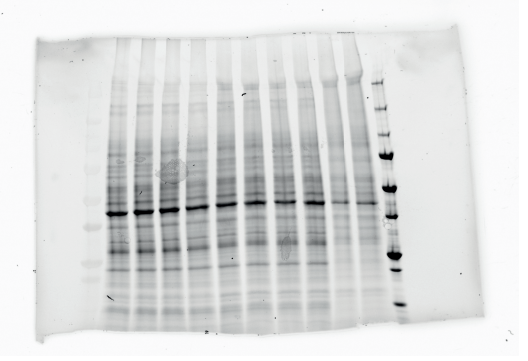

Blot 2 (P-Stat3 Ab)

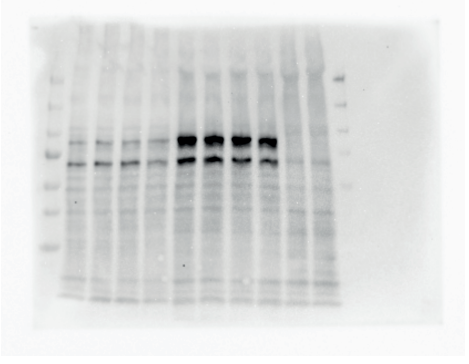

Image of Molecular Weight (MW) Marker

Blot 3 (NF-κB2 p100/p52 Ab)

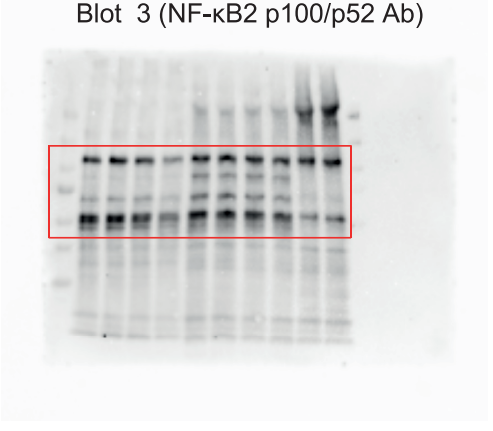

Full unedited blot and gel for Figure 3C

Blot (P-Stat3 Ab)

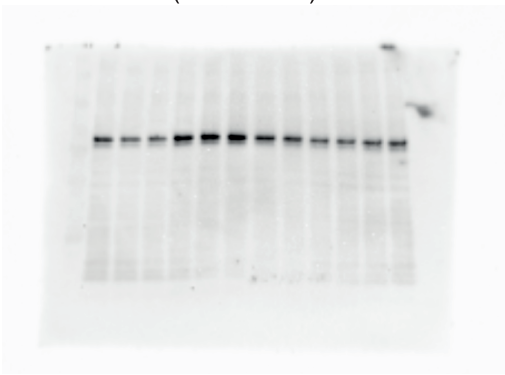

Image of Molecular Weight (MW) Marker

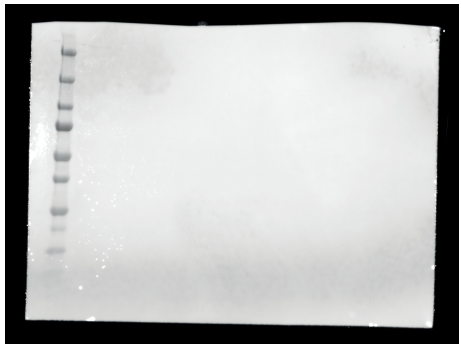

Gel (Total Protein)

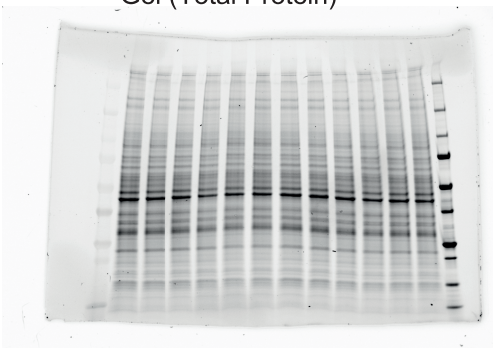

Full unedited blot and gel for Figure 3D

Blot (P-p65 Ab)

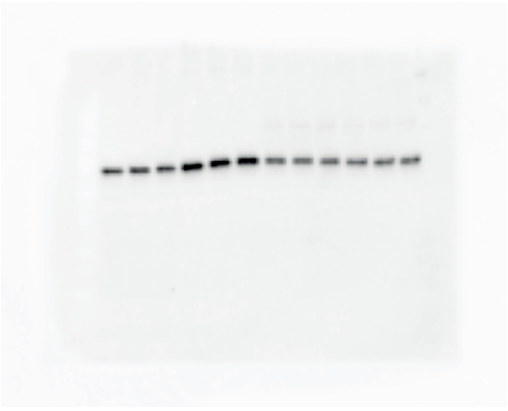

Image of Molecular Weight (MW) Marker

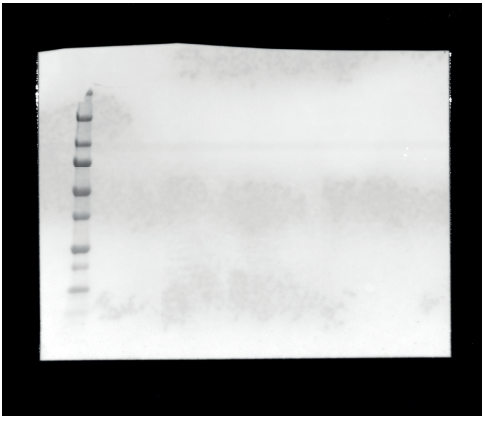

Gel (Total Protein)